



Strength requirements for shear diaphragms used for stability bracing of steel beams

O. Ozgur Egilmez¹, Mustafa Vardaroglu²

Abstract

Light gage metal sheeting is often used in steel building and bridge industries as concrete deck formwork. Besides providing support to the fresh concrete, sheeting acts like a shear diaphragm and provides continuous warping restraint to the top flanges of beams that they are attached to. Strength requirements of shear diaphragms bracing steel beams are not well established. A computational study was conducted to investigate the bracing behavior of shear diaphragms used to brace stocky and slender beams. This paper focuses on developing strength requirements for end and sidelap fasteners that connect deck sheets to structural members at the ends of the sheets and to each other at sidelap seams, respectively; and present results for stocky beams. To the best of the authors' knowledge this study is the first study that quantifies the stability induced fastener forces in sidelap fasteners. Doubly symmetric sections were considered. The effects of deck width and number of end and sidelap fasteners on brace forces were investigated. Expressions were developed to estimate the stability induced brace forces in end and sidelap fasteners.

1. Introduction

Lateral torsional buckling is a failure mode that often controls the design of steel I-beams during construction. During this critical stage, while the concrete is still wet and composite action has not started, the buckling capacity of the beams can be increased by reducing the laterally unbraced length by providing bracing at either discrete locations or continuously along the length of the beam. Light gage metal sheeting, which is often used in the building and bridge constructions as concrete deck formwork, acts like a shear diaphragm and can provide continuous lateral bracing to the top flange of non-composite beams by restraining the warping deformations along the beam span.

An adequate bracing system must have sufficient stiffness and strength to control deformations and brace forces (Winter 1960). Shear diaphragms possess a significant amount of stiffness and strength in the plane of the diaphragm. There have been a number of studies that investigated the stiffness and strength behavior of shear diaphragms used to brace steel beams (Helwig and Frank 1999, Helwig and Yura 2008a, b). These studies mainly focused on the strength of end connections

¹ Professor, Yasar University, <ozgur.egilmez@yasar.edu.tr>

² Research Assistant, University of Campania "Luigi Vanvitelli", <mustafa.vardaroglu@unicampania.it>

(sheet to beam connections along the length of the beams). However, the strength of a diaphragm is generally controlled by either the shear strength of end connections or shear strength of sidelap connections between panels (Luttrell 1981, Davies and Bryan 1982), both of which are generally achieved by mechanical fasteners. Therefore, strength requirements for shear diaphragm bracing should address both end and sidelap fasteners. Local and global buckling of the diaphragm, which are out of the scope of this study, are other possible failure modes (Luttrell 2004, Shimizu et al. 2013, Tong and Guo 2015) and should be checked in design.

A parametrical study was conducted to develop strength requirements for shear diaphragms used to brace stocky and slender beams at the construction stage. The end and sidelap fasteners that connect the diaphragm to top flanges of the beams and to each other, respectively, have been modeled separately. Detailed information on the finite element analytical (FEA) model used and its verification were discussed in Egilmez et al. (2014). This paper focuses on developing strength requirements for shear diaphragms bracing stocky beams. Strength requirements are developed for both end and sidelap fasteners. To the best of the authors' knowledge this study is the first study that quantifies the stability induced fastener forces in sidelap fasteners. This study targets mainly simply supported beams braced by shear diaphragms. For continuous beams, where the top flange near intermediate supports is under tension, the shear diaphragm bracing from deck sheets is not effective. Therefore, other sources of bracings will be required in the negative moment region to provide adequate stability bracing.

2. Previous Studies

There have been a number of research investigations on the bracing behavior of shear diaphragms. Extensive research on the buckling behavior of beams with shear diaphragm bracing was conducted during the 1960's and 1970's (Nethercot and Trahair 1975, Errera and Apparao 1976). These studies resulted in a relatively simple design expression for the buckling capacity of diaphragm-braced beams with uniform moment loading:

$$M_{cr} = M_g + 2Qe \quad (1)$$

where M_{cr} = buckling capacity of the diaphragm braced beam; M_g = capacity of the beam with no bracing; Q = shear rigidity of the deck; and e = distance from center of gravity of the beam to plane of shear diaphragm. Helwig and Frank (1999) presented finite element results that demonstrated the effects of moment gradient and load height on the bracing behavior of shear diaphragms used to brace slender beams with h/tw greater than 60. They modified the simplified uniform moment solution (Eq. (1)) to be applicable for general loading conditions and recommended the following expression to approximate the buckling capacity of steel beams braced by shear diaphragms:

$$M_{cr} = C_b^* M_g + mQd \quad (2)$$

where M_{cr} , M_g , and Q have been defined in Eq. (1); C_b^* = moment gradient factor that considers load height effects (Helwig et al. 1997, Zieman 2010); d = depth of the beam; and m = factor that depends on load position. Helwig and Frank (1999) recommended m values of 0.5 for loads applied at centroid and 0.375 for loads applied at top flange. In the late 2000's Helwig and Yura (2008a) extended the study of Helwig and Frank (1999) to stocky beams with h/tw less than 60. For stocky

beams Helwig and Yura recommended m values of 0.85 for centroid loading and 0.5 for top flange loading.

The expressions given in Eqs. (1)-(2) are applicable to a perfectly straight girder. Therefore, using such an equation to solve for the deck stiffness for a given moment would be analogous to the ideal stiffness requirement given by:

$$G'_i = \frac{Q_i}{s_d} = \frac{(M_u - C_b^* M_g)}{m d s_d} \quad (3)$$

where G'_i = effective ideal shear stiffness of diaphragm; Q_i = ideal shear rigidity of diaphragm; M_u = design moment along the beam; and other parameters have been defined in Eqs. (1)-(2). The brace stiffness required for a structural member to reach a specific load level or buckling capacity is often called the “ideal stiffness”. Helwig and Yura (2008b) also conducted large displacement analysis on shear diaphragm braced beams with h/t_w less than 60 to develop stiffness and strength requirements for shear diaphragms used to brace steel beams. In their study, the “ideal stiffness” of shear diaphragms was selected as the diaphragm stiffness from an eigenvalue buckling analysis that produced a maximum beam bending stress close to 345 MPa. Helwig and Yura (2008b) recommended providing four times the ideal stiffness to effectively control deformations and brace forces. Providing four times the ideal value results in the following expression:

Fig. 1 shows the free-body diagram of a deck sheet with four end fasteners and five sidelap fasteners. As depicted in Fig. 1 two force components develop at end fasteners: a) F_M , which is transverse to the beam longitudinal axis; b) F_V , which is parallel to the beam longitudinal axis. At sidelaps, only one force component develops, which is transverse to the beam longitudinal axis. The brace forces that develop at sidelap fasteners were ignored in Helwig and Yura’s (2008b) study. Helwig and Yura (2008b) assumed a linear distribution, which is symmetric with respect to the mid-span of a sheet, for the end fastener force components normal to the longitudinal axis (F_M). Shear forces (F_V) that develops along the width of the sheet were assumed to be equally resisted by each end fastener. The assumed orientations of the transverse (F_M) and longitudinal (F_V) fastener forces are depicted in Fig.1. Helwig and Yura (2008b) recommended the following expressions for FM and FV:

$$F_M = \frac{0.001 M_u L}{k d^2} \quad (4)$$

$$F_V = 2 \left(\frac{0.001 M_u L w_d}{L_d n_e d^2} \right) \quad (5)$$

where M_u = design moment that corresponds to a stress level of 345 MPa; L = spacing between discrete bracing points that prevent twist; d = depth of the section; L_d = length of the sheet; w_d = width of the sheet; n_e = number of end fasteners; and k = factor that depends on number of end fasteners. Helwig and Yura (2008b) recommended respective k values of 1.0, 1.0, 1.11, 1.25, and 1.38 for two, three, four, five, and six end fasteners. The resultant total fastener force can then be calculated as:

$$F_R = \sqrt{(F_M)^2 + (F_V)^2} \quad (6)$$

Helwig and Yura (2008b) also investigated the reduction in brace forces due to utilizing a stiffer brace than needed. They recommended the following coefficient, C_r , to be applied to Eq. (6) to calculate the reduced brace force due to a higher effective diaphragm stiffness provided than required ($G'_{req'd} = 4G'_i$).

$$C_r = \frac{3}{4} + \frac{1}{4} \left(\frac{G'_{req'd}}{G'_{prov}} \right)^2 \quad (7)$$

where G'_i = ideal effective stiffness of the diaphragm; $G'_{req'd}$ = required effective stiffness of the diaphragm; and G'_{prov} = provided effective diaphragm stiffness.

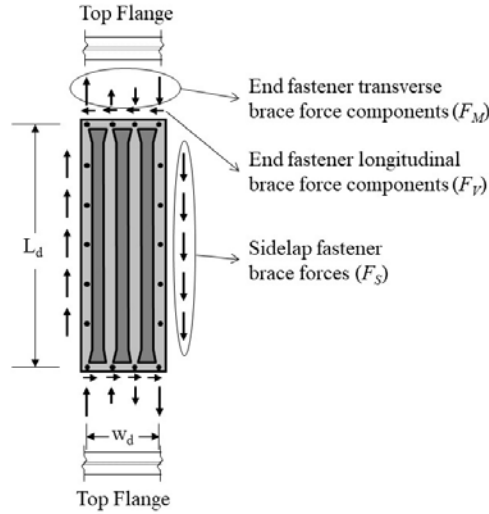


Figure 1: Free-body diagram of a single deck sheet

3. Finite Element Analytical (FEA) Model

3.1 FEA Model of Beams

The three-dimensional finite element program ANSYS (2007) was used to perform parametric studies on the behavior of steel I-beams braced by shear diaphragms. The FEA model consisted of a twin beam system with a shear diaphragm connected to the top flanges as depicted in Fig. 2. All of the elements used in the FEA model possessed linear elastic material properties. The beams and web stiffeners were meshed with 8-node shell elements. Two elements were used to model the flanges and four elements were used for the webs depending on the depth of the sections. The aspect ratio of the elements ranged between 1.2 and 2.0. The beams were simply supported with lateral movement prevented at the top and bottom flanges at the supports.

Initial imperfections play an important role in the magnitude of brace forces that develop in bracing members. Wang and Helwig (2005) showed that brace forces are directly proportional to the magnitude of initial imperfections for beams braced by cross frames or diaphragms. Wang and Helwig (2005) also showed that the worst-case imperfection for maximizing brace forces consists of a lateral sweep of the compression flange while the other flange remains essentially straight.

For the magnitude of lateral sweep of the top flange, both Wang and Helwig (2005) and Helwig and Yura (2008a) suggested using $L_b/500$, where L_b is the unbraced length of the beam, instead of the 1/1000 limit set by the AISC Code of Standard Practice (AISC 2010) on the variation in straightness between points of lateral supports in building applications. The reason for doubling the magnitude of lateral sweep is due to possible additional out-of-plumpness and uneven bearing supports in bridge constructions, which may result in larger imperfections. The same shape and magnitude recommended by Wang and Helwig (2005) and Helwig and Yura (2008a) for initial imperfections were adopted in this study and are shown in Fig. 2.

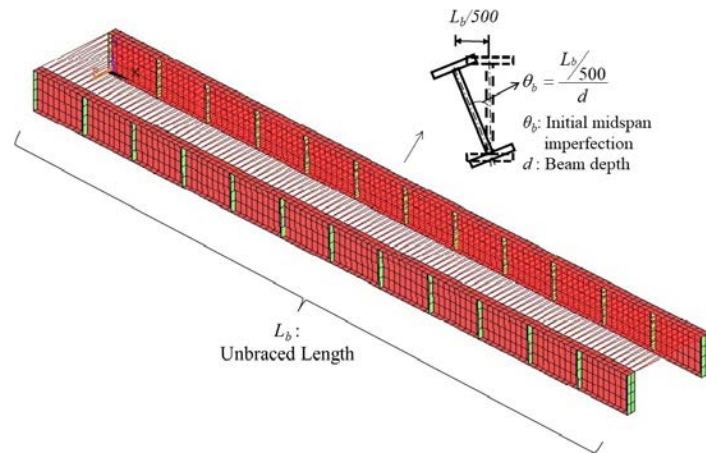


Figure 2: FEA model of twin-beams – shear diaphragm and beam initial imperfection

3.2 FEA Model Shear Diaphragm

As previously mentioned, steel deck forms are generally modelled as shear diaphragms that restrain the lateral movement of top flanges of steel beams that they are attached to. Deck forms that are commonly used in the construction industry consist of steel deck sheets with a cover length of 610 mm and 914 mm (Luttrell 2004, CANAM 2006). These steel deck forms are manufactured with different number of ribs. For example, the 610 mm wide steel decks are available in two, three, or four ribs. Steel decks with a cover length of 914 mm are generally manufactured with either three or six ribs. Since end fasteners are placed at the valley of the ribs, number of ribs in a deck form plays an important role in the arrangement of end fasteners. End fasteners can be placed in the valley of each rib, creating a fully fastened deck system; or at alternate valleys, creating a partially fastened deck system. The FEA model of the deck form sheet used in this study, which is explained below, enabled the width of the deck and number of end and sidelap fasteners to be easily changed. Strength requirements for shear diaphragms were initially developed by utilizing a model of the fully fastened 610 mm wide deck form sheet with three ribs, four end fasteners, five sidelap fasteners, and deck thickness of 1.52 mm. Additional analyses were then conducted with different deck width, number of end and sidelap fasteners, and deck thickness to investigate the effects of these parameters on the strength of end and sidelap fasteners.

Several FEA models of shear diaphragms are available in literature (Davies and Bryan 1982, Helwig and Frank 1999, Helwig and Yura 2008a, Galanes and Godoy 2014). The FEA model used in this study for shear diaphragms was originally developed by Davies and Bryan (1982) to investigate fastener forces resulting from lateral loading applied to building frames. In their study, Davies and Bryan (1982) simulated the shear stiffness of diaphragms by a series of bars forming

a truss as illustrated in Fig. 3. Each small truss shown in Fig. 3 consists of four transverse and three diagonal truss elements and represents a single deck sheet profile. As explained above, the deck sheet profile initially modeled in this study is a typical deck sheet with three ribs commonly used in both building and bridge applications. The transverse truss elements were located at every trough and spanned between the centerline of beam top flanges. This type of a representation of deck sheets enabled each deck to structural member fastener to be modeled by dimensionless spring elements and be placed at the ends of each transverse truss element. The transverse truss elements were connected to the beam top flange mid-nodes through dimensionless spring elements. The number of transverse truss elements could be changed depending on the number of fasteners used to connect the deck sheet to structural member. These truss elements were 3-D uniaxial tension-compression spar elements. The axial stiffness of the transverse elements was taken sufficiently high for their axial strain to be neglected. Hence, the shear stiffness of the deck sheets depended only on the properties of the diagonal elements. In order to determine the required area of the diagonal truss elements that correspond to a certain shear rigidity, an FEA model of a shear test frame was utilized.

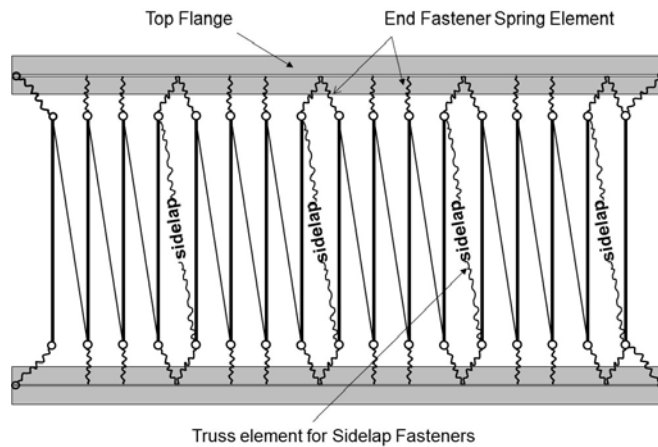


Figure 3: FEA model shear diaphragm

In both building and bridge forming systems deck sheets are generally fastened to supporting members along the ends and to each other at sidelaps by mechanical fasteners. Conventional mechanical fasteners for deck sheets are generally 19 mm long TEK screws with a 6.3 mm diameter. Deck sheet to structural member connections along the beam length were modeled by dimensionless spring elements that possess equal stiffness in two orthogonal directions, but no rotational stiffness. These spring elements were positioned at the centerline of beam top flanges and were connected to the mid-node of beam top flanges and the ends of the transverse truss elements as explained previously. Although the dimensionless spring elements are shown to have finite length in Fig. 3, this representation is merely for illustration purposes. In the actual model these spring elements were dimensionless. At sidelap locations along the beam length, separate spring elements were used to connect each transverse truss end to the same mid-node of beam top flange, as illustrated in Fig. 3. The transverse and lateral stiffness of these dimensionless spring elements represented the stiffness of deck sheet to structural member connections fastened by No. 12 and No. 14 Buildex TEK screws. The stiffness of such connections is given by Luttrell (2004). In the representation of shear diaphragm bracing systems, deck sheets adjacent to the supports were assumed to be fastened to structural members (beam, diaphragm, etc.) that span transversely

between the supports. The stiffness of these fasteners was also incorporated in the model by providing additional deck to structural member spring elements that connect the corner nodes of the deck trusses adjacent to the supports to the two beam mid-nodes at the supports.

Sidelap fasteners were modeled by a transverse truss element that connects opposite ends of adjacent small trusses as shown in Fig. 3. The stiffness of sidelap transverse truss elements represented the total stiffness of the number of sidelap fastener connections along the seam. TxDOT PMDF standards (TxDOT 2004) require a maximum center-to-center spacing of 450 mm at sidelaps. The number of fasteners at sidelap locations considered in this study ranged from six to two. Six and two fasteners correspond to deck lengths of approximately 3150 mm and 1350 mm, respectively. These deck lengths are in the upper limits of common deck lengths utilized in the building and bridge industries. The stiffness of one sidelap fastener connection was assumed to be the same as the stiffness of deck sheet to deck sheet connection fastened by No. 8 to No. 14 Buildex TEK screws; which is given by Luttrell (2004)

4. Overview of Study

Two doubly symmetric sections, with web slenderness ratios (h/t_w) of 60, were considered in the study. The depths of sections were 366 mm and 732 mm and they will be referred to as Stocky #1 and #2, respectively. The respective flange widths of Stocky #1 and #2 sections were 140 mm and 280 mm. Flange slenderness ratio (b/t_f) of these two stocky beams was 7.8. Span/depth (L/d) ratios of 15, 20, 25, and 30 were considered. The only loading considered was uniformly distributed loading applied at top flange. Uniformly distributed loading is representative of loading from poured concrete slab. Loading applied at mid-height was not considered since it is less critical as compared to top flange loading (Helwig and Yura 2008a).

As previously discussed, initial analyses were conducted utilizing the FEA model of a specific deck sheet. This specific deck sheet had a width of 610 mm with three ribs. The thickness of the deck sheet was taken as 1.52 mm. The deck sheet was assumed to be fully fastened to the beams at the ends by two fasteners at the corners and two between the ribs. The connections between individual deck sheets were assumed to be provided by five sidelap fasteners at each seam. As previously mentioned, TxDOT PMDF standards (TxDOT 2004) require a maximum center-to-center spacing of 450 mm at sidelaps. Therefore, five sidelap fasteners correspond to a deck length of 2700 mm, which is in the upper limits of deck lengths used in building and bridge applications. This specific deck sheet configuration will be referred to as the “standard deck sheet configuration” in the remainder of the paper. Strength requirements presented in this paper are initially developed for this standard deck sheet configuration for diaphragm rigidity of four times the ideal value (as recommended by Helwig and Yura, 2008b) and a stress level of 210 MPa. The effects of sheet thickness, sheet width, and number of end and sidelap fasteners are discussed separately in the following sections.

The design moment of the sections investigated in this study was taken as the moment corresponding to an in-plane bending stress equal to 210 MPa at the outer fiber of the section. The stress level of 210 MPa is somewhat arbitrary; however, it represents a reasonable level of in-plane bending stresses expected during construction. The property of shear diaphragms that is of interest for bracing purposes is the shear rigidity, which is denoted by the variable Q . For each section investigated in this study, the ideal shear rigidity (Q_i) was calculated by conducting an eigenvalue

buckling analysis on a perfectly straight twin-beam system braced by a shear diaphragm. The area of the diagonal truss elements of the shear diaphragm FEA model was calibrated to equate the eigenvalue of the twin-beam system to the moment level that creates a bending stress equal to 210 MPa at the outer fiber. An FEA model of shear test frame was then used to determine the ideal shear rigidity of the diaphragm that corresponds to the calibrated area of the diagonal truss elements. Large displacement analysis, which reflects the effects of geometrical imperfections, were then conducted on the twin-beam FEA model by using four times the ideal shear rigidity to observe deformations and brace forces.

5. FEA Results

5.1 Results for Standard Deck Sheet Configuration

In order to develop an expression to estimate the stability induced brace forces in end and sidelap fasteners, the maximum brace forces that develop along the length of the beams need to be identified. Brace forces that develop in a single deck sheet are shown in Fig. 1. The deck sheet shown in Fig. 1, which is the standard deck sheet configuration analyzed in this paper, has three ribs, four end fasteners, and five sidelap fasteners. As seen in Fig. 1 both transverse (F_M) and longitudinal forces (F_V) develop at end fasteners; whereas only transverse shear forces (F_S) develop at sidelap fasteners. The distribution of the resultant end fastener brace forces along the beam length for Stocky #1 and #2 sections with L/d of 25 and diaphragm rigidity of four times the ideal value is depicted in Fig. 4. The resultant forces shown in Fig. 4 were calculated by taking the square root of the summation of squares of the transverse and longitudinal force components that develop in each end fastener. Due to symmetry, the forces are shown over half the span. For L/d of 25 there were 7.5 and 15 deck sheets along half the beam lengths in Stocky #1 and Stocky#2 sections, respectively. Each curve shown in Fig. 4 belongs to a single deck sheet and each marker in a single curve shows the force in one out of four end fasteners in a single sheet. Maximum forces that developed in Stocky #2 sections were approximately four times higher than the forces that developed in Stocky #1 sections. Sections with L/d ratios of 15, 20, and 30 showed similar behavior.

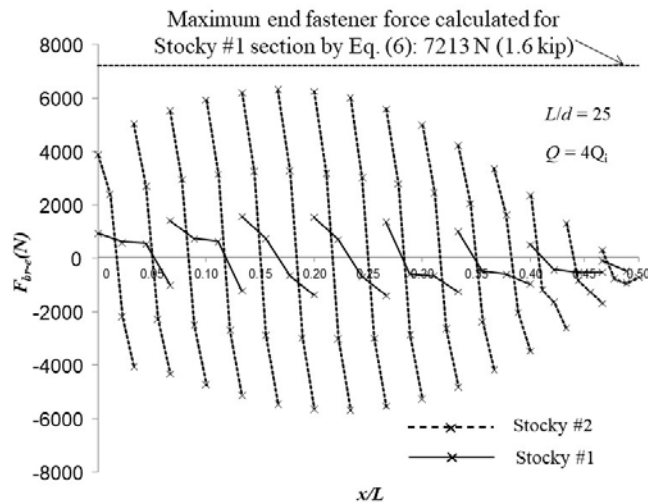


Figure 4: Distribution of resultant end fastener brace forces in each deck sheet

The horizontal lines to the top and bottom of the vertical axis in Fig. 4 indicate the magnitude of the maximum fastener force (7213 N) calculated by Eq. (6) (Helwig and Yura 2008b) for Stocky #1 section. This recommended value from literature (7213 N) is approximately 4.5 times higher than the maximum resultant fastener force observed in the analysis. Due to scale factors on the graph, the corresponding fastener force for Stocky #2 section (28855 N) calculated by Eq. (6) is not shown. For Stocky #2 section the recommended value from Eq. (6) was approximately 5 times higher than the maximum end fastener force obtained from the analysis. These significant differences in end fastener forces is mainly due to the fact that sidelap fasteners were not taken into account in Helwig and Yura’s (2008b) study and partly due to the fact that design stress levels were different in both studies (345 MPa in Helwig and Yura’s study compared to 210 MPa in this study).

Fig. 4 reveals that in a single deck sheet the maximum resultant end fastener brace force develops at edge fasteners, rather than at intermediate fasteners. A graph showing these maximum resultant end fastener forces in each deck sheet along half the beam length is provided in Fig. 5 for the two stocky sections for L/d ratios of 15, 20, 25, and 30. Due to symmetry, the forces are shown over half the span. The resultant end fastener forces were calculated by taking the square root of the squares of F_M and F_V . Each marker on the curves corresponds to the maximum resultant end fastener brace force (F_{br-e}) that develops in a single deck sheet along the length of the beam. These markers are located at the centerline of the deck sheets. Brace forces in the deeper Stocky #2 section were approximately 4 times higher than those in the shallower Stocky #1 section. The effect of L/d ratio on brace forces can also be observed in the figure. In both of the sections, maximum resultant end fastener brace forces increased as L/d ratio increased.

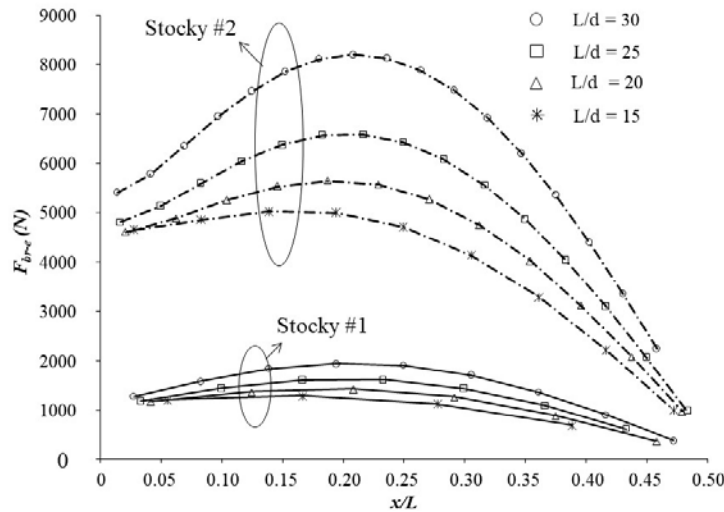


Figure 5: Distribution of maximum resultant end fastener brace forces in each deck sheet

Fig. 6 shows the distribution of sidelap fastener forces along half the beam length (due to symmetry) for Stocky #1 and #2 sections for a diaphragm rigidity of four times the ideal value. Results are presented for L/d of 15, 20, 25, and 30. As previously mentioned, sidelap fasteners were modeled using transverse truss elements. The stiffness of these transverse truss elements represented the total stiffness of the number of fasteners used at a sidelap seam. The markers shown in Fig. 6 correspond to the force in one sidelap fastener at each seam. The force in one sidelap

fastener was calculated by dividing the force that developed in the transverse truss elements to the number of sidelap fasteners at a seam. It was assumed that the force that developed at a sidelap seam was evenly distributed among the sidelap fasteners along the seam. For both of the sections sidelap fastener forces increased as L/d ratios increased. The increase in brace forces as L/d ratios increase, were much more significant in Stocky #2 sections, as compared to the difference in force levels observed in Stocky #1 sections for different L/d ratios. The forces that developed in Stocky #2 section were approximately 3 to 5 times higher than the forces that developed in Stocky #1 sections.

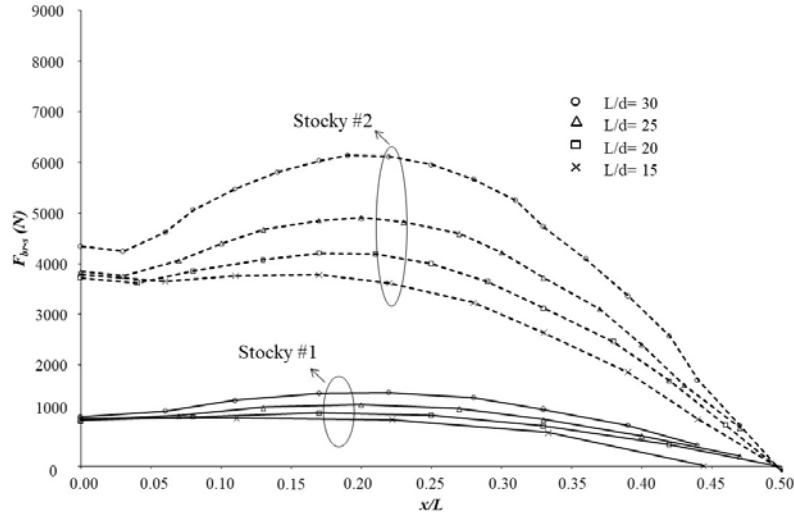


Figure 6: Distribution of maximum sidelap fastener brace forces at each seam

In order to achieve a direct comparison between the maximum resultant end fastener brace forces of the two stocky sections with different L/d ratios, the maximum resultant end fastener brace forces presented in Figs. 5 and 6 were normalized by the maximum applied beam moment, M_u , and the ratio of L/d^2 ; similar to the normalization procedure followed by Helwig and Yura (2008b). The resultant curves are presented in Figs. 7 and 8 for end and sidelap fastener brace forces; respectively. Although there were significant differences in magnitudes of the maximum end fastener brace forces of the two sections (as seen in Fig. 5), the normalized curves shown in Fig. 7 coincide for L/d ratio of 15, 20, and 25. For example for both Stocky #1 and Stocky #2 sections the respective maximum normalized end fastener brace forces were approximately 0.000268, 0.000222, and 0.000207 for L/d ratios of 15, 20, and 25. For L/d ratio of 30, the respective maximum normalized end fastener brace forces were 0.000215 and 0.000204 for Stocky #2 and Stocky #1 sections. The normalized curves presented in Fig. 7 also indicate that maximum normalized brace forces tend to decrease as L/d ratio increases. The only exception was Stocky #2 section with $L/d = 30$, which had a higher maximum normalized brace force than sections with $L/d = 25$.

An identical normalization procedure was followed for sidelap fastener brace forces and the resultant curves are presented in Fig. 8. Similar to the curves for maximum normalized end fastener brace forces, the maximum normalized sidelap fastener brace force curves also coincide for L/d ratio of 15, 20, and 25. For example for both Stocky #1 and Stocky #2 sections the respective maximum normalized sidelap fastener forces were approximately 0.000204, 0.000172, and

0.000162 for L/d ratio of 15, 20, and 25, respectively. The maximum normalized sidlap fastener brace force for Stocky #2 section with $L/d = 30$ was 0.000168, which was slightly higher than that of sections with $L/d = 25$; and the maximum normalized sidlap fastener force for Stocky #1 section with $L/d = 30$ was 0.000159. Based upon the results presented in Figs. 7 and 8 conservative estimates of the maximum normalized end and sidlap fastener brace forces for stocky sections can be taken as 0.0003 and 0.00025, respectively.

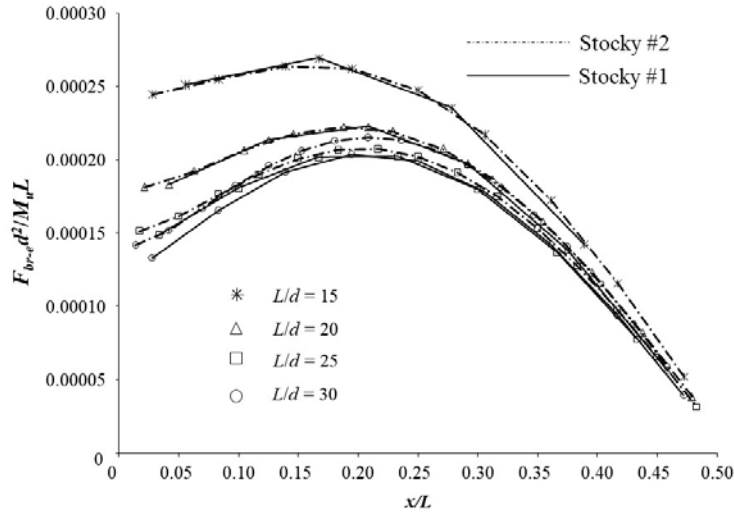


Figure 7: Maximum normalized end fastener brace forces

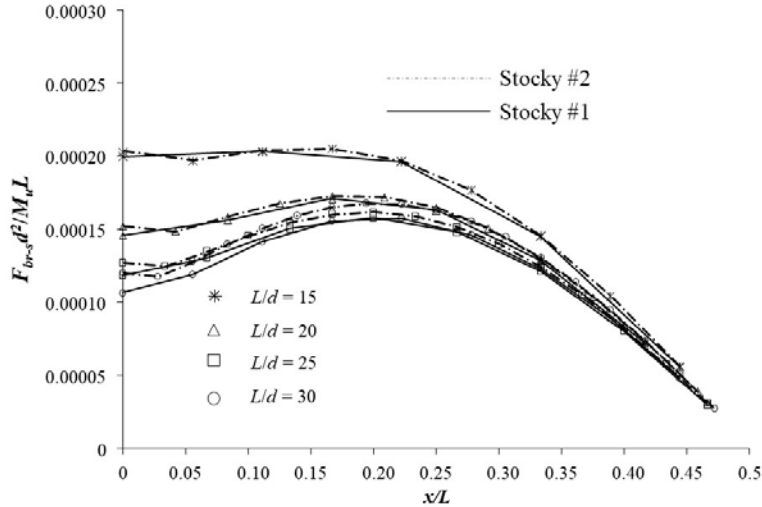


Figure 8: Maximum normalized sidlap fastener brace forces

5.2 Effects of Deck Sheet Thickness, Deck Width, and Number of Fasteners on Brace Forces

As previously explained, the conservative estimates of maximum normalized end and sidlap fastener brace force values recommended above were determined for the standard deck sheet configuration. This standard deck sheet configuration possessed a sheet thickness of 1.52 mm, deck width of 610 mm, four end and five sidlap fasteners; which is a typical deck sheet commonly used in the construction industry (Luttrell 2004, CANAM 2007). Additional large displacement analyses were conducted on the two sections with different sheet thicknesses, deck widths, and

number of end and sidelap fasteners to investigate the effects of these parameters on end and sidelap fastener brace forces.

The maximum normalized end and sidelap fastener brace force values recommended in the previous section was based on the results of the section with the highest normalized brace force among all the stocky and slender sections analyzed. For example, the section that possessed the highest maximum normalized end and sidelap fastener brace force values was Stocky #1 section with $L/d = 15$. Since this section was the section with the highest normalized brace forces, due to space limitations, the effects of sheet thickness, deck width, and number of end and sidelap fasteners on normalized brace forces will be demonstrated by showing results from only this section. Normalized brace forces that developed in Stocky #2 section were smaller than those developed in this section.

Fig. 9 shows a graph of maximum normalized end and sidelap fastener force distribution along half the beam length for Stocky #1 section with $L/d = 15$ for sheet thicknesses of 1.52 mm, 1.21 mm, and 0.91 mm. Deck width and number of end and sidelap fasteners were kept the same as in the standard deck configuration. Only half of the beam length is shown since brace forces are symmetric with respect to mid-span. The maximum normalized end and sidelap fastener brace forces were almost coincident for the three diaphragm thicknesses. The results indicate that magnitude of brace forces are independent of diaphragm thickness.

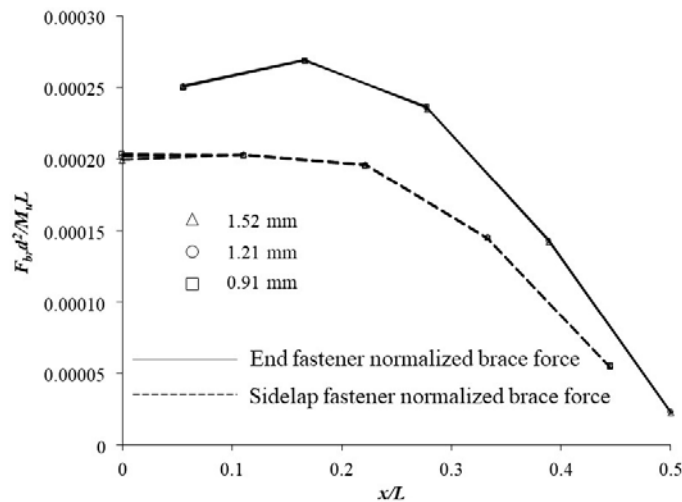


Figure 9: Effect of deck thickness on brace forces

A graph of variation in maximum normalized end and sidelap fastener brace forces in Stocky #1 section with $L/d = 15$ with respect to deck width is provided in Fig. 10. Results are shown for two different deck widths: 610 mm and 914 mm. Deck sheets that are commonly used in the construction industry consist of deck sheets with a cover length of 610 mm and 914 mm (Luttrell 2004, CANAM 2006). Sheet thickness and number of end and sidelap fasteners were kept the same as in the standard deck configuration. Keeping the number of end fasteners the same while increasing the width of the deck to 914 mm, corresponds to a partially fastened 914 mm wide deck sheet with six ribs. For such a system, the four end fasteners will be placed at alternate valleys of the ribs. While the maximum normalized end fastener brace forces were 0.000269 and 0.000294

for deck widths of 610 mm and 914 mm, respectively; increasing the deck width to 914 mm while keeping other parameters the same, did not have a significant effect on maximum normalized sidelap fastener brace forces. For both deck widths maximum normalized sidelap fastener brace forces were approximately 0.000204. Based upon the results presented in Fig. 10, the respective recommended values of 0.0003 and 0.00025 for maximum normalized end and sidelap fastener brace forces do not need to be modified for the increase in deck width.

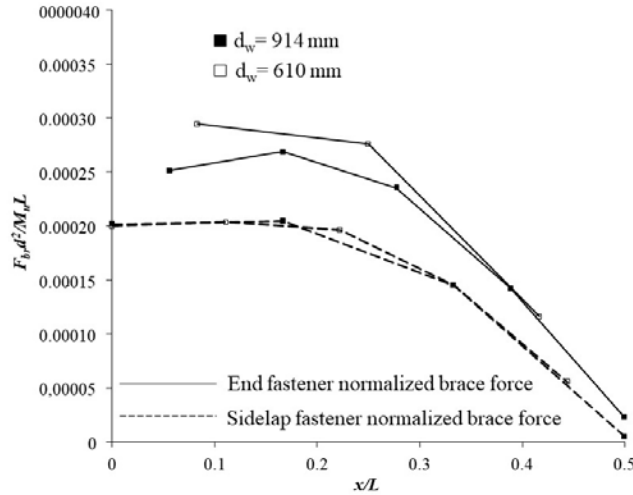


Figure 10: Effect of deck width on brace forces

As explained above, a 914 mm deck sheet with four end fasteners represents a partially fastened deck system. However, designers might prefer to specify a fully fastened deck system no matter what the width of the deck sheet is, since the deck systems are relied upon for stability bracing. Therefore, additional analyses were conducted for a fully fastened deck system with 914 mm wide deck sheets with six ribs; which are fastened to the top flanges of steel beams by seven end fasteners through each valley of the ribs. Although not shown in Fig. 10, for such systems, maximum normalized end and sidelap fastener brace forces were smaller than those of the fully fastened 610 mm wide deck system with four end fasteners for both sections.

Fig. 11 shows a graph of the distribution of maximum resultant end fastener and sidelap fastener brace forces along half the beam length for Stocky #1 section with $L/d = 15$ for deck systems with three, four, and five end fasteners. Sheet thickness, deck width, and number of sidelap fasteners were kept the same as in the standard deck sheet configuration. The maximum normalized end fastener brace forces of Stocky #1 section increased as the number of end fasteners decreased. For Stocky #1 section maximum normalized end fastener brace forces were 0.000252, 0.000269, and 0.00305 for five, four, and three end fasteners. However, the same trend in brace forces was not observed for maximum normalized sidelap fastener brace forces. The normalized sidelap fastener brace forces did not change due to a decrease or increase in number of end fasteners. Based upon the results presented in Fig. 11, the respective recommended values of 0.0003 and 0.00025 for maximum normalized end and sidelap fastener brace forces do not need to be modified for the change in number of end fasteners.

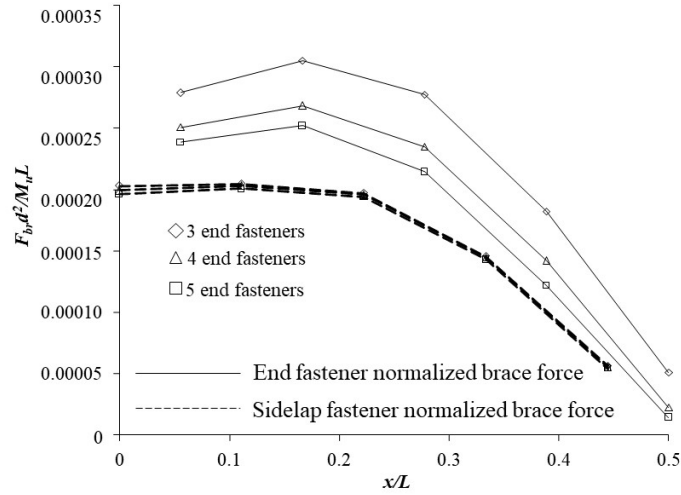


Figure 11: Effect of number of end fasteners on brace forces

Fig. 12 shows the effect of number of sidelap fasteners on the distribution of maximum end and sidelap fastener brace forces along half the beam length for Stocky #1 section with $L/d = 15$. Five different number of sidelap fasteners were used: two, three, four, five, and six. The curves presented in Fig. 12 indicate that brace forces increase as number of sidelap fasteners decrease. The respective maximum resultant end fastener brace forces were 0.000244, 0.000269, 0.000301, 0.000347 and 0.000415; and respective maximum resultant sidelap fastener brace forces were 0.000179, 0.000203, 0.000235, 0.000279, and 0.000347 for six, five, four, three, and two sidelap fasteners. Based upon the results presented in Fig. 12, conservative estimates of the maximum normalized end and sidelap fastener brace forces of slender sections can be taken as 0.00045, 0.00035, 0.00030, 0.00030, 0.00025 and 0.00035, 0.00030, 0.00025, 0.00025, 0.00020 for two, three, four, five, and six sidelap fasteners, respectively.

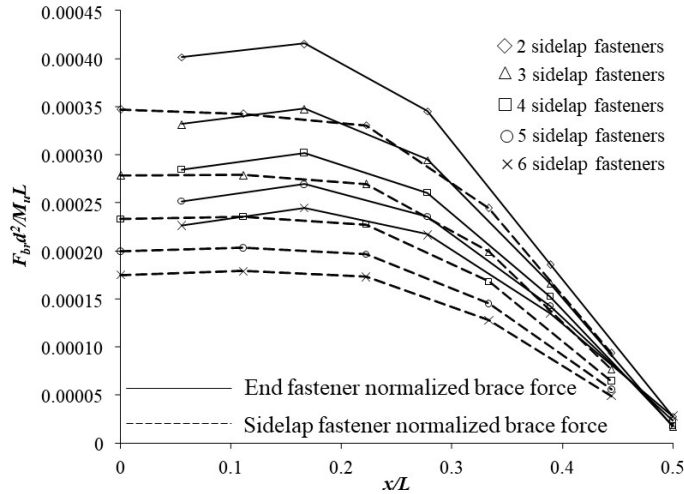


Figure 12: Effect of number of sidelap fasteners on brace forces

6. Diaphragm Strength Requirements

Based upon the results presented in the preceding section, the following expressions can be used to obtain reasonable estimates of maximum end and sidelap fastener forces for shear diaphragms used to brace stocky beams:

$$F_{br-e} = C_r s_e k_e w_e \frac{M_u L}{d^2} \quad (8)$$

$$F_{br-s} = C_r s_s k_s w_s \frac{M_u L}{d^2} \quad (9)$$

where F_{br-e} = maximum end fastener brace force; F_{br-s} = maximum sidelap fastener brace force; C_r = reduction coefficient that depends on the provided diaphragm stiffness given by Eq. (7), s_e and s_s = factors that depend on number of sidelap fasteners; k_e and k_s = factors that depend on number of end fasteners; w_e and w_s = factors that depends on deck width; M_u = maximum design moment; L = spacing between discrete brace points that prevents twist; and d = depth of the section. Recommended values of s_e and s_s , k_e and k_s , and w_e and w_s are presented in Tables 1 through 3, respectively.

Table 1: Effect of number of sidelap fasteners on brace forces

# of Sidelap Fasteners	s_e	s_s
2	0.00045	0.00035
3	0.00035	0.00030
4	0.00030	0.00025
5	0.00030	0.00025
6	0.00025	0.00020

Table 2: Effect of number of end fasteners on brace forces

# of End Fasteners	k_e	k_s
3	1.0	1.0
4	1.0	1.0
5	1.0	1.0

Table 3: Effect of deck width on brace forces

# of End Fasteners	k_e	k_s
610 ^{mm} with 4 end fasteners	1.0	1.0
914 ^{mm} with 4 end fasteners	1.0	1.0
914 ^{mm} with 7 end fasteners	1.0	1.0

The values in Table-2 correspond to deck systems with four end fasteners. Additional analyses were conducted on 610 mm wide deck systems with three and five end fasteners that possessed two, three, four, and six sidelap fasteners and on 914 mm wide deck systems with three and five

end fasteners that possessed two, three, four, five, and six sidelap fasteners. The results indicated that the values provided in Table-2 are also applicable to such systems.

As previously noted, Eqs. (8)-(9) are based upon the stiffness requirement ($Q_{req'd} = 4Q_i$) recommended by Helwig and Yura (2008b) and the imperfection magnitude of $\theta_o = (L/500d)$. In building applications design provisions permit smaller initial imperfections to be adopted in design (AISC 2016a). In such cases, the expressions in Eqs. (8) and (9) can be reduced proportionally (Wang and Helwig 2005). Providing a diaphragm stiffness higher than the required value results in a reduction in brace forces (Helwig and Yura 2008b). Helwig and Yura (2008b) recommended using a reduction coefficient, C_r , given in Eq. (7) to estimate the reduction in brace forces due to higher brace stiffnesses than needed. Additional large displacement analyses were conducted on the twelve sections with diaphragm stiffnesses of $5Q_i$, $6Q_i$, $7Q_i$, and $8Q_i$ to obtain a measure of the reduction in maximum end and sidelap fastener forces. It was observed that Eq. (7) gives reasonable estimates for reductions in both end and sidelap fastener forces.

Eqs. (8)-(9) were developed for a twin-beam system. In a twin beam system, there is sheeting on only one side of the beams; therefore the diaphragm braces two beams. For a system with multiple beams brace forces can be reduced significantly since there will be sheeting on both sides of the beams. Egilmez et al. (2016) recommended using the following expression to quantify the reduction in brace forces due to multiple beams braced by deck sheeting:

$$N_g = \frac{0.5n}{(n-1)} \quad (10)$$

where N_g = reduction coefficient due to multiple beams braced by deck sheets; n = number of beams braced by deck sheeting. Eqs. (8) and (9) can be multiplied by the reduction factor N_g to obtain reasonable estimates of brace forces for systems with multiple beams. For exterior beams there will be sheeting on only one side of the beam. Therefore, the reduction factor N_g should not be used for exterior girders. However, for exterior beams with little or no overhangs, the loading can be substantially smaller.

If the LRFD format is used in design, M_u should be the factored design moment and the strength of the end fastener connection and sidelap fastener connection should be reduced by a resistance factor, ϕ , of 0.65 (Luttrell 2004). If the ASD format is used in design, M_u should be based on service level loads and the strength of the end fastener connection and sidelap fastener connection should be reduced by a factor of safety, Ω , of 2.5 (Luttrell 2004). Designers can use equations provided by the SDI Manual (Luttrell 2004) to calculate the strength of end and sidelap fastener connections. A design example is provided in Appendix that demonstrates the application of stiffness and strength requirements.

The strength of a diaphragm can also be governed by local or global buckling of the diaphragm. These failure modes should also be checked in design. The stability induced fastener forces can be combined with loads from other sources, such as lateral loading, to check the local and global buckling strength of shear diaphragms using expressions from literature (Luttrell 1981, Davies and Bryan 1982).

7. Conclusions

This paper is the second part of a two-part paper that presents results from a computational study on the strength behavior of shear diaphragms used for stability bracing of stocky steel beams. Expressions were developed that can be used to determine the stability induced end and sidelap fastener brace forces. To the best of the authors' knowledge this study is the first study that focuses on stability induced sidelap fastener forces in literature. The results indicate that brace forces depend on the number of end and sidelap fasteners, width of the diaphragm, and web slenderness ratio.

Appendix

Design Example

Flooring System: Consists of a series of eight W460 × 106 girders spanning 15 m. The tributary width of deck bracing a single beam is 2.4 m. The only bracing that is relied on during construction is the metal deck sheets; there is no intermediate discrete bracing system. Determine the thickness of the deck sheet that will be used to provide stability bracing to interior beams during concrete cast. During concrete casting, the beam is subjected to a maximum factored moment of 416 kN-m. This moment level corresponds to a construction stress level of 200 MPa and is less than $\phi M_r = 517$ kN-m; the upper limit of elastic behavior (AISC 1999).

Girder Properties: L_b = unbraced length = 15 m; d = depth = 469 mm; I_y = moment of inertia in the y-y axis = 25.1×10^6 mm⁴; J = torsional constant = 1460×10^3 mm⁴; C_w = warping constant = 1260×10^9 mm⁶; $F_y = 345$ MPa.

Check Lateral Torsional Buckling of Beam with $L_b = 15$ m: Although self-weight of the girder acts at mid-height, the majority of the load is applied at the top flange (construction loads and fresh concrete). Assume the entire load is applied at the top flange. Due to top flange loading moment gradient factor, C_b , should be modified as follows: $C_b^* = C_b/1.4$ (Helwig et al. 1997). For top flange uniform distributed loading C_b can be taken as 1.14 (Ziemian 2010). Therefore $C_b^* = C_b/1.4 = 1.14/1.4 = 0.81$. Assuming elastic buckling, the capacity of the girder can be obtained by the following expression (Timoshenko and Gere 1961):

$$\phi M_n = \phi C_b^* M_b = \phi C_b^* \frac{\pi}{L_b} \sqrt{EI_y GJ + \frac{\pi^2 E^2 C_w I_y}{L_b^2}} = 118.8 \text{ kN} - \text{m}$$

Brace Stiffness Requirement:

Use Eq. (3) to calculate the ideal effective shear stiffness of the metal deck sheet bracing system:

$$G'_{ideal} = \frac{(M_u - \phi C_b^* M_b)}{m d s_d} = \frac{(416^{kN-m} - 118.8^{kN-m})}{2.4^m \times 0.5 \times 0.469^m} = 528 \frac{\text{kN}}{\text{m}} / \text{rad}$$

Use four times the ideal value to control deformations and brace forces:

$$G'_{req'd} = 4G'_{ideal} = 4 \times 528 \frac{\text{kN}}{\text{m}} / \text{rad} = 2112 \frac{\text{kN}}{\text{m}} / \text{rad}$$

A diaphragm with an effective shear stiffness of 2112 kN/m/rad should be provided. Expressions provided in the Steel Deck Institute Diaphragm Design Manual (Luttrell 2004) can be used to select an appropriate diaphragm. For example a diaphragm with a panel length of 2440 mm, panel width of 2440 mm, deck sheet thickness of 0.91 mm, deck sheet width of 610 mm, deck sheets fastened to the top flanges of the beams at each rib and at the corners by four fasteners, deck sheets fastened to each other by five fasteners at sidelaps has an effective shear stiffness of 4293 kN/m/rad. Apply a ϕ factor of 0.65 to the provided stiffness value:

$$\phi G'_{prov} = 0.65 \times 4293 \frac{\text{kN}}{\text{m}/\text{rad}} = 2790 \frac{\text{kN}}{\text{m}}/\text{rad} > G'_{req'd} = 2112 \frac{\text{kN}}{\text{m}}/\text{rad} \text{ O.K.}$$

Brace Strength Requirement:

Eqs. (8) and (9) can be used to obtain reasonable estimates of maximum end and sidelap fastener brace forces. These expressions were developed for a twin-beam system where the diaphragm was bracing two beams. For a system with multiple beams these expressions can be modified by the reduction factor N_g :

$$F_{br-e} = N_g C_r s_e k_e w_e \frac{M_u L}{d^2} = 0.57 \times 1.0 \times 0.0003 \times 1.0 \times 1.0 \times \frac{416^{\text{kN-m}} \times 15^{\text{m}}}{(0.469^{\text{m}})^2} = 4.85 \text{ kN}$$

$$F_{br-s} = N_g C_r s_s k_s w_s \frac{M_u L}{d^2} = 0.57 \times 1.0 \times 0.00025 \times 1.0 \times 1.0 \times \frac{416^{\text{kN-m}} \times 15^{\text{m}}}{(0.469^{\text{m}})^2} = 4.1 \text{ kN}$$

where $N_g = 0.5 \times 8 / (8-1) = 0.57$; $s_e = 0.0003$ (Table 1); $k_e = 1.0$ (Table 2); $w_e = 1.0$ (Table 3); $s_s = 0.00025$ (Table 1); $k_s = 1.0$ (Table 2); $w_s = 1.0$ (Table 3); $M_u = 416 \text{ kN-m}$; $L =$ spacing between discrete bracing points that prevent twist = 15 m; and $d =$ depth of beam = 0.469 m. Provided effective diaphragm stiffness, $G'_{prov} = 2790 \text{ kN/m/rad}$, is slightly higher than $G'_{req'd} = 2112 \text{ kN/m/rad}$. C_r can be taken as 1.0 for simplicity.

These brace force expressions were based on an initial imperfection of $\theta_o = L/(500d)$. In most building applications an initial imperfection of $\theta_o = L/(1000d)$ is deemed appropriate. Therefore, the above estimated brace forces can be reduced by half and compared by the shear strength of the fastener connections. The shear strength of a deck sheet to structural member fastener connection with mechanical fasteners, such as No. 12 and No. 14 screws, is given by Luttrell (2004):

$$Q_t = \frac{F_y t}{31.5} \left(1 - \frac{F_y}{1380}\right) \text{ (kN)} \quad \text{SDI Eq. 4.5-1 (Luttrell, 2004)}$$

where $F_y =$ yield strength of sheet metal = 235 MPa; and $t =$ sheet metal thickness = 1.21 mm

$$\phi Q_t = 0.65 \frac{235^{\text{MPa}} \times 1.21^{\text{mm}}}{31.5} \left(1 - \frac{235^{\text{MPa}}}{1380}\right) = 4.86 \text{ kN} > F_{br-e} = 4.85 \text{ kN OK.}$$

The shear strength of a sheet to sheet fastener connection at sidelaps is given by Luttrell (2004):

$$Q_s = 0.793 dt \text{ (kN)} \quad \text{SDI Eq. 4.5-2 (Luttrell, 2004)}$$

where d = major diameter of the screw (mm); and t = sheet metal thickness = 1.21 mm. Assuming No. 12 TEK screws is used:

$$\phi Q_s = 0.65 \times .793 \times 12^{\text{mm}} \times 1.21^{\text{mm}} = 7.48 \text{ kN} > F_{br-s} = 4.1 \text{ kN OK.}$$

A diaphragm system with 1.21 mm thick, open end (with three corrugations), 75×200 (75 mm depth, 200 mm pitch) metal deck forms with a 610 mm cover width can be used to brace the W460 × 106 beams during construction. The local and global buckling capacity of the diaphragm should also be check before finalizing the design of the bracing system.

References

- AISC, (1999), *Manual of steel construction, metric conversions of the second edition*, Chicago.
- AISC, (2016), *Code of standard practice for steel buildings and bridges*, 15th Ed., Chicago.
- ANSYS, (2007), *Finite Element Model Users Manual*, (Version 11.0), ANSYS Inc., Canonsburg, Pa, USA.
- CANAM, (2007), *Steel Deck Diaphragm Catalogue*, Boucherville.
- Davies J.M., Bryan E.R. (1982). *Manual of Stressed Skin Diaphragm Design*, JW&S, NY, USA.
- Egilmez, O.O., Helwig, T.A., and Herman, R. (2016). "Using metal deck forms for construction bracing in steel bridges," *Journal of Bridge Engineering*, ASCE, 21(5).
- Egilmez, O.O., Vardaroglu, M., Ababa, A. (2014). "Stiffness and strength of shear diaphragms used for stability bracing of slender beams." *Proceedings of the Annual Stability Conference*, Structural Stability Research Council, Toronto, Canada, March 25-28, 230-245.
- Errera, S. and Apparao, T. (1976), "Design of I-shaped beams with diaphragm bracing", *Journal of the Structural Division*, 102(4), 769-781.
- Galanes, O. R. and Godoy, L. A. (2014), "Modeling of wind-induced fatigue of cold-formed steel sheet panels", *Structural Engineering and Mechanics*, 49(2), 237-259.
- Helwig, T. A. and Frank, K. H. (1999). "Stiffness requirements for diaphragm bracing of beams," *Journal of Structural Engineering*, ASCE, 125(11), 1249-1256.
- Helwig, T. A., Frank, K. H., and Yura, J. A. (1997), "Lateral-torsional buckling of singly-symmetric I-beams", *Journal of Structural Engineering*, 123(9), 1172-1179.
- Helwig, T. A., Yura, J. A. (2008a). "Shear diaphragm bracing of beams. I: Stiffness requirements," *Journal of Structural Engineering*, ASCE, 134(3), 348-356.
- Helwig, T. A., Yura, J. A. (2008b). "Shear diaphragm bracing of beams. I: Design requirements," *Journal of Structural Engineering*, ASCE, 134(3), 357-363.
- Luttrell, L. D. & Steel Deck Institute (1981). *Steel Deck Institute diaphragm design manual*, 1st Ed., MO.
- Luttrell, L. D. (2004). *Steel Deck Institute diaphragm design manual*, 3rd Ed., Canton, Ohio.
- Nethercot, D. and Trahair, N. (1975), "Design of diaphragm-braced I-beams", *Journal of the Structural Division*, 101(10), 2045-2061.
- Shimizu, N., Kanno, R., Ikarashi, K., Sato, K., and Hanya, K. (2013), "Cyclic behavior of corrugated steel shear diaphragms with end failure", *Journal of Structural Engineering*, 139 (Special issue on cold form steel structures), 796-806.
- Texas Department of Transportation (TxDOT) (2004), *Permanent Metal Deck Form Standards*, TxDOT Bridge Division, Texas, WA.
- Timoshenko, S.P. and Gere, J.M. (1961), *Theory of elastic stability*, Dover Publications, New York, USA.
- Tong, J. Z. and Guo, Y.L. (2015), "Elastic buckling behavior of steel trapezoidal corrugated shear walls", *Thin-Walled Structures*, 95(October), 31-39.
- Wang, L. and Helwig, Todd A. (2005), "Critical imperfections for beam bracing systems", *Journal of Structural Engineering*, 131(6), 933-940.
- Winter, G. (1960). "Lateral bracing of columns and beams." *Trans. Am. Soc. Civ. Eng.*, 125, 809-825.
- Ziemian, R., ed. (2010), *Guide to Stability Design Criteria for Metal Structures*, 6th Ed., JW & S, USA.